

## Harmonic generation in Taylor vortices between rotating cylinders

By H. A. SNYDER AND R. B. LAMBERT

Brown University, Providence, Rhode Island

(Received 25 October 1965 and in revised form 9 March 1966)

A theory of finite-amplitude secondary flow between concentric rotating cylinders has been published by Davey (1962). A necessary feature of the theory is the generation of harmonics of the spatial periodicity in the axial direction of the velocity field. A method has been devised to measure the amplitude of each harmonic separately and experimental results for the fundamental and first three harmonics are presented here for Taylor numbers up to 100 times the critical value. The agreement with Davey's theory is excellent, and the agreement extends far beyond the range where the theory is expected to be valid. It is shown that all the harmonics are in phase with the fundamental. This result requires that jets and shock-like structure must be present in the velocity field.

---

### 1. Introduction

The nature of the flow régime between the laminar region and the region of fully developed turbulence, commonly termed secondary or transitional flows, is very poorly understood. Most of the work in this area of research both theoretical and experimental is concentrated on studying either the first transition from laminar flow or the turbulent region. Yet for many applications in geophysics and probably many in engineering also, the régime is that of secondary flow.

Due to the complexity of the problem, it is best to confine investigations of transitional flows to situations where the boundary conditions have a high order of symmetry. Not all cases are admissible, for it is possible for the velocity field to change directly from the laminar to the turbulent condition without any intervening secondary (e.g. circular Poiseuille flow). The arrangement which has the simplest geometry and yet has an extended region of transition consists of concentric rotating cylinders. This is the famous Taylor double-cylinder problem (Taylor 1923). The research described below is an experimental investigation of the Taylor problem (circular Couette flow) in the region above the first transition.

Considerable theoretical work has been applied in studying circular Couette flow. Linearized stability theory has been used to predict the transition to the first secondary mode for various conditions of rotation, various clearance ratios, and for several additional imposed conditions, such as axial flow. Theory, in each case, also predicts the wave-form and wavelength of the disturbance at transition. The experimental results are in excellent agreement with the theory in every instance. Linear stability as applied to the Taylor problem has been reviewed thoroughly by Chandrasekhar (1961) and more recently by Di Prima (1963).

When the amplitude of secondary flow becomes finite and the linearized theory ceases to hold, the non-linearity of the governing equations has prevented theoretical progress in all problems of this sort from being either rapid or widespread. However, a few investigations based on a perturbation from the linearized solution have been successful in predicting the observed results so long as these are confined to the vicinity of the neutral curve. At present the most notable theoretical paper which presents quantitative results on the finite-amplitude Taylor problem is by Davey (1962). The calculations of Davey are based on methods developed by Stuart (1958, 1960) and by Watson (1960).

The features of the stability problem which are the results of non-linearity are: the distortion of the mean velocity profile; and the generation of harmonics of the spatial periodicity. Davey (1962) computed the distortion of the mean, the amplitude of the velocity field of the fundamental Taylor vortex, and the amplitude of the first harmonic for three cases: (1) a wide gap with only the inner cylinder rotating; (2) a narrow gap with only the inner cylinder rotating; and (3) a narrow gap with the outer cylinder rotating at nearly the speed of the inner cylinder. He has assumed that the disturbances are axisymmetric. In the case of the narrow gap this assumption is true only a few per cent above the neutral curve. Therefore, cases (2) and (3) cannot be expected to agree well with experiment except very close to the critical Taylor number  $T_c$ . To the authors' knowledge, Davey's case (1) is the only quantitative prediction of finite-amplitude effects for the double-cylinder apparatus which can be expected to agree with experiment over an extended range. The data presented in this paper shows that Davey's calculations are in excellent agreement with experimental observations. In fact the agreement is good far beyond the range of Taylor numbers over which the theory might be expected to apply.

Several experimental investigations reported in the literature bear on the present problem. Coles (1965) has shown that secondary flow occurs over a large range of Taylor numbers and that the prevalent wave-form in a narrow gap has azimuthal dependence. He has also shown that hysteresis can occur between transitions from one wave-form to another.

The distortion of the mean flow may be measured by observing the torque on one of the cylinders. Torque measurements have been reported by Wendt (1933), by Taylor (1936), and by Donnelly (1958). The available data has been compiled and critically compared in a review by Donnelly & Simon (1960). Davey has compared his computations with the torque data of Donnelly (1958) and finds good agreement.

The other predicted quantities of the theory, the amplitudes of the fundamental and the harmonics, have been tested in part by Donnelly & Schwartz (1965) using the ion method. This instrument measures the radial component of the velocity field at the outer cylinder. The work carried out with the ion technique may be considered incomplete in three aspects: first, the published results apply to a narrow-gap apparatus where the onset of non-axisymmetric modes follows close above the neutral curve. It will be shown in a subsequent paper that the amplitude of circulation in a Taylor cell in the vicinity just below the onset of a new mode is strongly affected by the anticipation of the transition.

In the reference under consideration, the region of influence of the wave transition includes as much as half the range investigated. The case of a wide gap where this difficulty is not encountered is not reported because the ion current becomes too small to measure.

Secondly, the ion method gives a relative—not absolute—indication of the velocity. Quoting in part from Donnelly & Schwartz (1965): ‘Since the charge of the double layer,  $Q$  is not known independently, we have made no attempt to assess the absolute magnitude of  $A_e$  or its variation from one set of cylinders to another. Daily variations in sensitivity made such absolute comparisons completely unreliable’. Accordingly, the data obtained by the ion method must be fitted to the predicted curve at one point.

Finally, the velocity amplitudes measured by the ion method have not been analysed into Fourier components. The quantity which is shown on the graphs of Donnelly & Schwartz (1965) as  $A_e$  is the total peak-to-peak amplitude of the velocity profile as the detector is moved axially through one wavelength. As long as the amplitude is small,  $A_e$  accurately represents the amplitude of the fundamental, but when distortion due to higher harmonics is evident,  $A_e$  (as used by Donnelly & Schwartz 1965) no longer agrees with the definition used by Davey (1962). The peak-to-peak amplitude may be either larger or smaller than the fundamental depending on the phase difference of the harmonics.

In the research reported here the measuring instrument is the hot thermistor anemometer developed by the authors (Lambert, Snyder & Karlsson 1965). The output of this device is related to the total shear relative to the surface where the detector is located. It is possible to calibrate the anemometer in absolute units. This instrument has been used to measure the amplitude of the fundamental and the three lowest harmonics of the spatial periodicity of Taylor vortices. For all the data presented here, the ratio of the radii of the inner to outer cylinder  $R_1/R_2$  is one-half. Only the inner cylinder is rotated, the range of Taylor numbers is up to  $100T_c$ , where  $T_c$  is the critical number for the onset of secondary flow.

The body of this report includes a section outlining the relevant parts of Davey’s theory, a section on the equipment and its calibration, an explanation of the data taking and data reduction procedure, a description of the results, and finally a discussion of the results in terms of jets and shock waves. Some preliminary results of this research have been published (Lambert, Snyder & Karlsson 1964).

## 2. Summary of the theory

Davey (1962) uses the full non-linear equations of motion and assumes the velocity is axisymmetric and periodic in  $z$ . Using a method similar to that of Stuart (1960) and Watson (1960), Davey shows that there is a formal expansion of each of the components in powers of a time-dependent function  $A(t)$  multiplied by a function of the radial co-ordinate. Thus, each component of the velocity is completely separable in terms of its independent variables. The amplitude function is itself determined by a series

$$\frac{1}{A} \frac{dA}{dt} = \sigma + a_1 A^2 + a_2 A^4 + \dots \quad (2.1)$$

In the limit of small  $A$ ,  $A \propto e^{\sigma t}$  so that  $\sigma$  is the amplification rate of the linearized problem. The coefficients  $a_m$  are constants. If the series for the velocity components is carried to order  $A^{2m}$ , the parameter that must be small for the expansion to converge is  $m\sigma$ . To first order  $A_e$ , the equilibrium value of  $A(t)$  as  $t \rightarrow \infty$ , has the value  $A_e^2 = (-\sigma/a_1)\{1 + O(A_e^2)\}$ .

In cylindrical co-ordinates  $(r, \theta, z)$  with the rotational axis in the  $z$ -direction, the velocity components  $(u, v, w)$  have the form

$$\begin{aligned} v = & v(r) + A^2 f_1(r) + A^4 f_2(r) + \dots + A\{v_{10}(r) + A^2 v_{11}(r) + A^4 v_{12}(r) + \dots\} \cos \lambda z \\ & + A^2\{v_{20}(r) + A^2 v_{21}(r) + \dots\} \cos 2\lambda z \\ & + A^3\{v_{30}(r) + \dots\} \cos 3\lambda z + \dots, \end{aligned} \quad (2.2)$$

where the laminar flow is written  $v(r)$ , the terms in  $f_n(r)$  represent the distortion of the mean motion, and  $\lambda$  is the wave-number of the disturbance. Note that the axial periodicity of the linearized solution requires that the non-linear terms in the motional equations generate spatial harmonics of the basic periodicity. The functional form of the  $u$  component is similar to  $v$  except that the terms  $v(r)$  and  $f_n(r)$  are omitted. The  $w$  component is like  $u$  except that the axial dependence is in  $\sin n\lambda z$  instead of  $\cos n\lambda z$ .

The infinite set of differential equations which results from inserting equations (2.1), (2.2), and the corresponding expansions for  $u$  and  $w$  into the equations of motion involves, after some reduction,  $u_{nm}(r)$ ,  $v_{nm}(r)$  and  $f_n(r)$ . Fortunately, the perturbation scheme is consistent so that the data necessary to solve the  $n$ th order set of equations is provided by the next lower order. Davey (1962) has computed  $u_{10}$ ,  $v_{10}$ ,  $u_{20}$ ,  $v_{20}$ , and the first three derivatives of each together with  $f_1$  and its first derivative. In calculating these functions to first order in  $\sigma$  (as Davey has done) it is within the approximation to take  $\sigma = 0$  and this procedure has been followed. Davey's computations are complete to order  $\sigma$  and provide a prediction of the distortion of the mean, the amplitude of the fundamental disturbance, and the amplitude of the first harmonic to order  $A_e^2$ . For fixed  $R_1/R_2$ ,  $\Omega_2/\Omega_1$ , and  $\lambda$ , both  $A_e$  and  $\sigma$  are functions only of the Taylor number. Davey has shown that with  $R_1/R_2 = \frac{1}{2}$ ,  $\Omega_2/\Omega_1 = 0$ , and  $\lambda = 3.163/R_1$  (the wave-number of the linear theory) that the critical Taylor number is  $T_c = 33,062$ ,

$$\sigma = 13.44(1 - T_c/T), \quad (2.3)$$

and

$$A_e^2 = 0.09017(1 - T_c/T). \quad (2.4)$$

The Taylor number for the problem has been defined as

$$T = (64/9) (\Omega_1/\nu)^2 R_1^4. \quad (2.5)$$

How far above  $T_c$  this theory is applicable will be discussed later.

The anemometers used in these experiments are sensitive to the shear at the wall. To compare our data with that of Davey (1962) we must find the total shear at  $r = R_1$  (the location of the anemometer). The shear has two components, and from equation (2.2) and a similar equation for  $w$  we find:

$$\left( \frac{\partial v}{\partial r} - \frac{v}{r} \right) = \frac{\nu R}{R_1^2} \left\{ -\frac{5}{3} + A_e^2 f_1 + A_e \frac{\partial v_{10}}{\partial r} \cos \lambda z + A_e^2 \frac{\partial^2 v_{20}}{\partial r^2} \cos 2\lambda z \right\}, \quad (2.6)$$

$$\frac{\partial w}{\partial r} = -\frac{\nu R}{R_1^2} \left\{ A_e \frac{\partial^2 u_{10}}{\partial r^2} \sin \lambda z + \frac{1}{2} A_e^2 \frac{\partial^2 u_{20}}{\partial r^2} \sin 2\lambda z \right\}, \quad (2.7)$$

and the total shear is

$$S = \left[ \left( \frac{\partial v}{\partial r} - \frac{v}{r} \right)_{R_1}^2 + \left( \frac{\partial w}{\partial r} \right)_{R_1}^2 \right]^{\frac{1}{2}}, \quad (2.8)$$

where  $\nu$  is the kinematic viscosity and  $R$  is the Reynolds number ( $R = \Omega_1 R_1^2 / \nu$ ).

Using the tables of Davey (1962) and equations (2.6) to (2.8) we have computed  $S$  for a fixed value of  $A_e$  at 28 equally spaced values of  $z$  throughout one period of  $z$ . The resulting curve is Fourier analysed and recorded. This procedure is applied to successive values of  $A_e$  and the result is a table of Fourier components of the shear as functions of  $A_e$ . From equation (2.4) and these tables the graphs of the theory used below are formed.

It should be noted that  $S$  can be made dimensionless by scaling with  $1/\Omega_1$ , thus,  $S/\Omega_1$  is independent of the dimensions of the apparatus and the fluid used. The measurable shear scales as  $\nu/R_1^2$ . We have presented our results for the generation of harmonics in the form of a Fourier series as follows:

$$S/\Omega_1 = \sum_{n=0}^{\infty} A_n \cos n\lambda z. \quad (2.9)$$

The values of  $A_n$  and  $\lambda$  as functions of  $T$  are the quantities measured and reported in the next sections. It is not possible to write a simple relation between the  $A_n$ 's and  $A_e$  which will hold when  $(T - T_c)/T$  is not small: in comparing our results with the predictions we have not attempted to calculate  $A_e$  from the  $A_n$ 's because of the inordinate amount of computations which are necessary. The good agreement with Davey's prediction (1962) of the shear shows that the value he used for  $A_e$  and the assumed solution must be correct.

### 3. Equipment

#### 3.1. Description

The rotating cylinder apparatus and the temperature control system were described in a previous paper, Snyder & Karlsson (1964). It is sufficient, then, to list the parameters which enter into the following computations. The radii of the inner and outer cylinders are  $R_1 = 3.140 \pm 0.002$  cm and  $R_2 = 6.295 \pm 0.002$  cm respectively, and the length of the cylinders is 90 and 95 cm respectively.

All data were taken under isothermal conditions and the temperature was maintained at  $24.5^\circ\text{C}$ . The maximum difference in temperature between any pair of thermal baths was kept to less than  $0.02^\circ\text{C}$ . Thermal gradients of this order of magnitude are not expected to affect the result significantly, Snyder & Karlsson (1964, 1965), Karlsson & Snyder (1965). To prevent appreciable zero drift of the thermistor response the long-term thermal stability of the working fluid must be about  $\pm 0.003^\circ\text{C}$ . This degree of regulation was achieved over periods of  $\frac{1}{2}$  h.

The fluid consisted of solutions of glycerol. The kinematic viscosity was varied from 0.009 to 0.215 Stokes using different ratios of glycerine and water. Before and after each set of readings with a particular fluid, the viscosity was measured with a Cannon-Fenske viscometer.

The design and operating characteristics of the anemometers and the associated circuitry together with the theory of their operation have already been reported by Lambert *et al.* (1965). There are three thermistors located on the outer surface of the inner cylinder. Two are at the same horizontal level at 30 cm from the bottom of the inner cylinder and are separated in arc by  $45^\circ$ ; the other is in a vertical line 2.30 cm above one of the lower thermistors. Three channels of electronics are operated simultaneously and the outputs are recorded in synchronism so that phase shifts may be measured conveniently. The Taylor cells are swept past the detector with a small axial flow (axial Reynolds number of order one). This arrangement makes it possible to infer the axial drift rate, the azimuthal drift rate, the azimuthal wave-number, and the wavelength of the cells from the recorder tracer.

### 3.2. Calibration

The theory of operation of the anemometer has been worked out by Niiler (1965) and has been modified for the particular application described here by Lambert *et al.* (1965). Let  $\Delta T$  represent the excess temperature of the thermistor above the ambient at a distance far from the thermistor when there is not shear. Also, let  $\delta T$  represent the change in  $\Delta T$  due to shear. Then it is shown in the latter reference that

$$\delta T / \Delta T = a S_{\text{surface}}^{\frac{1}{2}}. \quad (3.1)$$

The constant  $a$  is known in terms of the properties of the fluid and the thermistor (see equation (7) of Lambert *et al.* 1965). However, equation (3.1) holds only when  $S$  is sufficiently large; but for all data reported in this paper, this condition is fulfilled.

Calibration of the anemometer requires knowledge of three constants, each of which must be evaluated at the operating point: (1) the constant  $a$  of equation (3.1); (2) the sensitivity of the thermistor,  $\gamma = \delta R / R \delta T$  where  $\delta R$  is the change in resistance of the thermistor; and (3) the total gain of the electronic system  $k_1$ , from the input to recorded output.

The electronic gain is easily measured by first balancing the bridge (see figure 2 of Lambert *et al.* 1965), and then measuring the deflexion of the recorder for various settings of the decade resistance box. The curve relating the recorder deflexion to the out of balance resistance is linear to within 1% over the range used in these experiments and the slope is  $k_1$ . The value of  $k_1$  is checked at intervals of about 1 h while the apparatus is in operation. The gain varies by less than 3% from hour to hour.

The sensitivity of the thermistor is the slope of the resistance *vs* temperature curve at the operating point. We have calculated  $\gamma$  from known characteristic curves and the value for the thermistor which is used for quantitative data is  $\gamma = 1144/K^\circ$ .

To find  $a$  it is necessary first to find  $\Delta T$  for various inputs of power. Knowing  $k_1$  and  $\gamma$ , it is possible to measure  $\Delta T$  *vs* power input by noting the recorder deflexion for various values of current to the thermistor. These measurements are carried out with the fluid at rest. Heating curves have been drawn for two cases: when the fluid is (1) a 72% glycerine in water solution; and (2) air. Both

curves are linear to within 1% to well above the operating range. The slope in case (1) is 0.335 °C/mW and in case (2) is 0.370 °C/mW. We can conclude from the small difference of the slopes between curves (1) and (2) that most of the heat is conducted to the wall and only a small fraction (about 2 mW out of 18 mW) to the fluid. In deriving equation (10) of Lambert *et al.* (1965), it is assumed that most of the heat flows to the wall.

Having determined  $k_1$ ,  $\gamma$ , and  $\Delta T$ , it is possible to find  $a$  by measuring the recorder deflexion for different amounts of shear. The calibration is made in the region of laminar flow where the shear can be calculated. A large range of shear with laminar profile can be achieved if both cylinders are rotated. The resulting curve of  $\delta T/\Delta T$  vs  $S$  is linear on a log-log plot with a slope of 1/3. The curve is linear to about 2% except for small values of  $S$  where the assumptions made in deriving equation (3.1) are violated. The value of  $a$  depends upon the properties of the fluid and it can be shown that for two different fluids  $a \propto kP^{1/3}$ , where  $k$  is the thermal conductivity of the fluid and  $P$  is its Prandtl number. We have determined  $a$  empirically from the curves representing equation (3.1).

Typical values of the design parameters at our operating point are:

(a) total power input, 18 mW; (b) power transmitted to the fluid, 2 mW; (c) excess temperature  $\Delta T = 6$  °C; (d)  $S$  just below critical, 4/sec; (e) limit of applicability of equation (3.1),  $S = 3$ /sec; (f)  $a \approx 2.4 \times 10^{-2}$ .

## 4. Procedure

### 4.1. Data taking

At the beginning of each run the temperatures of the three thermal baths are adjusted so that the apparatus is isothermal at 24.5 °C. The speed of the inner cylinder is set to correspond to the desired value of the Taylor number. The axial flow is fixed to give an axial Reynolds number ( $R_x = \bar{V}R_1/\nu$  where  $\bar{V}$  is the average velocity) of 2.25. The same value of  $R_x$  is maintained for all the runs. Taylor cells are swept past the anemometer by the axial flow and the recorder responds to the changing value of the shear. Figure 1 shows some actual recorder traces.

The signal to the recorder can be digitalized by a voltage-to-frequency converter and counter. The digitalized output is displayed on a print out and may be transferred to punched cards for entry into a computer. After the recorder trace has been steady for about 2 min, sections of the trace are recorded in digital form. The standard procedure is to print out six complete cycles of the wave-form for each Taylor number.

The outputs of all three anemometers are recorded continuously and simultaneously. It is necessary to synchronize the time base of the three traces about once an hour. A continuous record of the temperature at various points in the thermal baths is also maintained. The raw data consists of the six cycles of recorder trace from one of the anemometers which has been digitalized (for each Taylor number), the three recorder traces, the dimensions of the apparatus, and the properties of the fluid.

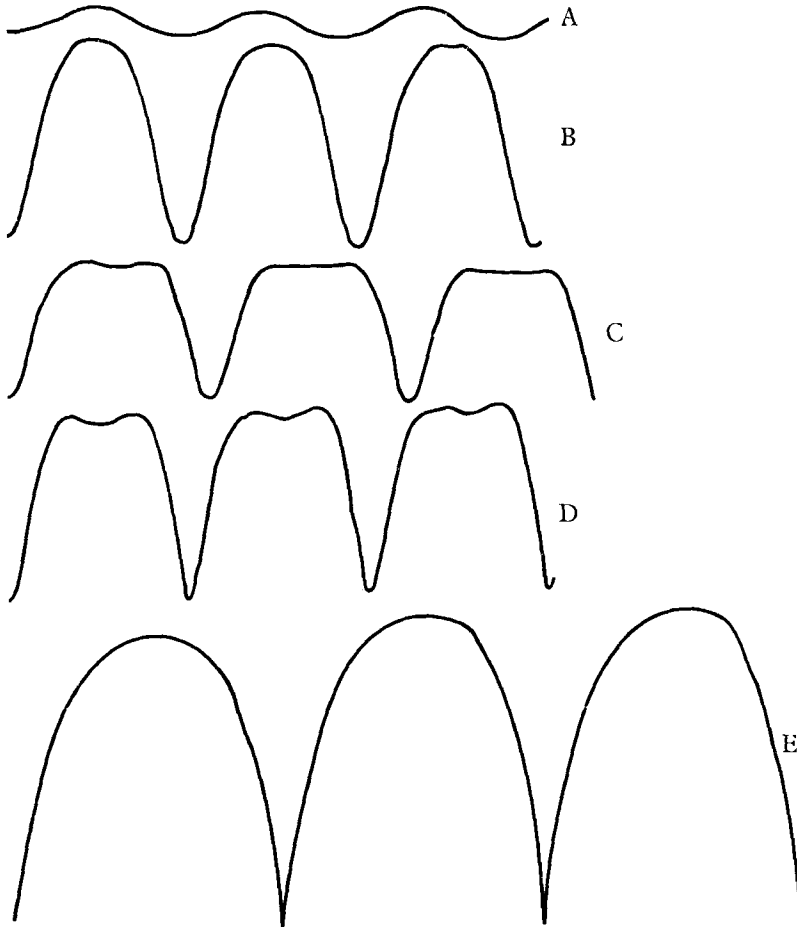


FIGURE 1. Recorder traces of the total shear at the inner cylinder at increasing values of the Taylor number. The cells are moved past the detector. Values of  $(1 - T_c/T)$  are: (A) 0.02, (B) 0.09, (C) 0.43, (D) 0.70, and (E) 0.99. The amplitude scale is 1/2 for (C) through (E).

#### 4.2. *Data reduction*

The wavelength of the disturbance is determined by comparing the recorder traces of the two anemometers which are in a vertical line. The distance between the anemometers is less than a wavelength of the disturbance. If the phase difference of the two traces is measured in time units as  $t_1$  and the distance between the two detectors is  $l$ , then the drift velocity of the disturbance is  $V_d = t_1/l$ . Note that  $V_d$  is not necessarily equal to  $\bar{V}$  since the disturbance is a wave motion. The velocity  $V_d$  can be combined with the time  $t_2$  required for a complete cycle to pass either anemometer to yield the wavelength of the disturbance:  $2\pi/\lambda = V_d t_2$ . Generally, the points on the graphs of  $\lambda$  which follow, are the average values of six determinations.

The first step in finding the harmonic amplitudes of the wave-form is to convert the digitalized recorder output into values of shear. There is usually a long-term



drift of the zero point of the recorder due to drifts in the mean temperature of the working fluid. Therefore, only the a.c. part of the output is used in the calculations. Thus,  $\delta T$  which is directly proportional to the recorder deflexion is made up of two parts:  $\delta T = \delta T_{\text{a.c.}} + \delta T_{\text{d.c.}}$ . It is necessary to know  $\delta T_{\text{d.c.}}$  since the relation between the shear and  $\delta T$  is not linear and the range of  $\delta T$  is large enough so that a linear approximation is inappropriate. Fortunately, it is possible to calculate  $\delta T_{\text{d.c.}}$  from published data. We have from equation (3.1)

$$\delta T_{\text{d.c.}}/\Delta T = a |\bar{d}\bar{v}/dr - \Omega_1|^{\frac{1}{2}}, \quad (4.1)$$

where  $\bar{v}$  is the mean value of  $v$ . The quantity  $|\bar{d}\bar{v}/dr - \Omega_1|$  is measured by the torque. Therefore, it is possible to compute  $|\bar{d}\bar{v}/dr - \Omega_1|$  as a function of the Taylor number from the formulae supplied by Donnelly & Simon (1960) and this is the procedure that has been used.

It is also possible to measure  $\delta T_{\text{d.c.}}/\Delta T$  with the thermistor anemometer. First, the bridge is balanced with no rotation of the cylinder and the recorder zero is noted. Then, the cylinder is set into rotation. The resulting trace has a mean value which is offset from the previous recorder zero by an amount proportional to  $\delta T_{\text{d.c.}}/\Delta T$ . The method of this paragraph eliminates the cumulative zero shift due to long-term temperature drift. Several points were checked in this manner and were found to be in good agreement with the torque data. We plan to use this method to check the torque data more completely in the near future.

The a.c. part of the recorder deflexion  $D$  is related to  $\delta T_{\text{a.c.}}$  as  $\delta T_{\text{a.c.}} = (k_1/\gamma)D$  while  $\delta T_{\text{d.c.}}$  is given by equation (4.1). If equation (3.1) is rewritten as

$$S = (a\Delta T)^{-3} (\delta T_{\text{a.c.}} + \delta T_{\text{d.c.}})^3 \quad (4.2)$$

it is evident that all the information needed to find  $S$  is on hand. Both  $a$  and  $\Delta T$  may be found from calibration curves as explained in §3.

The next step is to Fourier analyse  $S$  with a computer. Since there is always some noise mixed with the output signal and also a long-term drift of the zero point, the question arises whether it is possible to reduce the effects of either or both these undesirable features by judicious data handling. The level of noise can be estimated and reduced by treating  $N$  cycles of the recorder trace as a single cycle in the computer analysis. If the recorder signal contained no noise, all Fourier components of the computer analysis would be zero except those whose subscripts were multiples of  $N$ . The magnitude of the components which are multiples of  $N$  relative to those that are not, is a measure of the signal-to-noise ratio.

The effect of the noise on the computed Fourier components is dependent to some extent on the number of data points used per cycle. As the number of points is increased, the effect of the noise level is decreased. However, the relation is far from linear and there is a point of diminishing return. The choice of  $N$ , the number of recorder traces in each computer cycle, and the total number of digitalized points (determined by the sampling rate) was determined empirically. Several traces were analysed with varying sampling rates and with  $N = 2, 3$ , and 4. By comparing the results we conclude that for the noise level of our apparatus it is sufficient to take  $N = 2$  and to use a total of fifty points in each analysis.

The standard procedure for reducing the data has been to use  $N = 2$  and to set the sampling rate so that there is a minimum of fifty data points for one computer cycle. Since the sampling rate is maintained constant, the number of points per analysis may range up to ninety as the wavelength increases. Sufficient trials have been made to show that the results are not appreciably effected by the number of points used, provided there are at least fifty in a complete cycle. The effect of the zero drift has been reduced by subtracting from each data point a quadratic function fitted to the three minimum points of the trace. (The trace is considered to begin and end at a minimum point; this is the point in the cell of maximum shear.)

The computer program consists of: (1) averaging the points on the trace and subtracting the average value from each point; (2) fitting a quadratic to the three minima and subtracting this function from each point; (3) multiplying each point by  $k_1/\gamma$ ; (4) calculating  $|\partial\bar{v}/\partial r - \Omega_1|^\frac{1}{2}$  and  $\delta T_{a.c.}$  from tables supplied; (5) adding  $\delta T_{a.c.}$  to  $\delta T_{d.c.}$  and using the result according to equation (4.2) to find  $S$ ; and (6) Fourier analysing  $S$ . The fundamental and first three harmonics are desired. Accordingly, the computer prints out both in-phase and out-of-phase components up to subscript 9, together with useful quantities such as the Taylor number, etc. The even components represent the desired Fourier analysis of the shear while the odd components measure the noise level. Each computer analysis is checked for noise content by comparing the magnitude of the odd and out-of-phase components with the fundamental. If the signal-to-noise level is less than ten, the analysis is repeated with new data. Since a total of six recorder cycles are digitalized for each Taylor number, there is a possibility of three computer analyses on the same data. Generally, two out of the three are processed and if the even components agree to within 10%, they are averaged and constitute a data point. If agreement is poor the analysis is rejected.

## 5. Data

The wave-number of the disturbance stays fairly constant throughout a large range of Taylor numbers. A plot of the wave-number  $\lambda$  scaled by the gap width  $R_1$  is shown in figure 2; there is a slight decrease at large values of  $T$ . The systematic errors in  $\lambda$  are considerably smaller than the statistical scatter. The fact that the wavelength of the disturbance is not very reproducible from run to run is well known (Snyder 1962); the spread found here is of the same magnitude reported by others. The uncertainty in  $\lambda$  can be taken as the extent of scatter shown on the graph.

The Fourier amplitudes of the shear as defined in equation (2.9) are plotted in figures 3–7. Referring to equation (4.2) it will be seen that the errors in the Fourier amplitudes may be quite large because the measured quantities are cubed. We can estimate the error in  $\delta T$  as about 3% from the scatter; the systematic error is less than 1%. The uncertainty due to scatter in the data is all statistical error. An error in  $a\Delta T$  of about 3% is estimated if  $a$  is calculated from its defining equation. However, this quantity can also be found empirically by measurements in the laminar region. The latter procedure has been carried out and we estimate a systematic error of  $1\frac{1}{2}\%$  in  $a\Delta T$ . The error in each point of  $S$

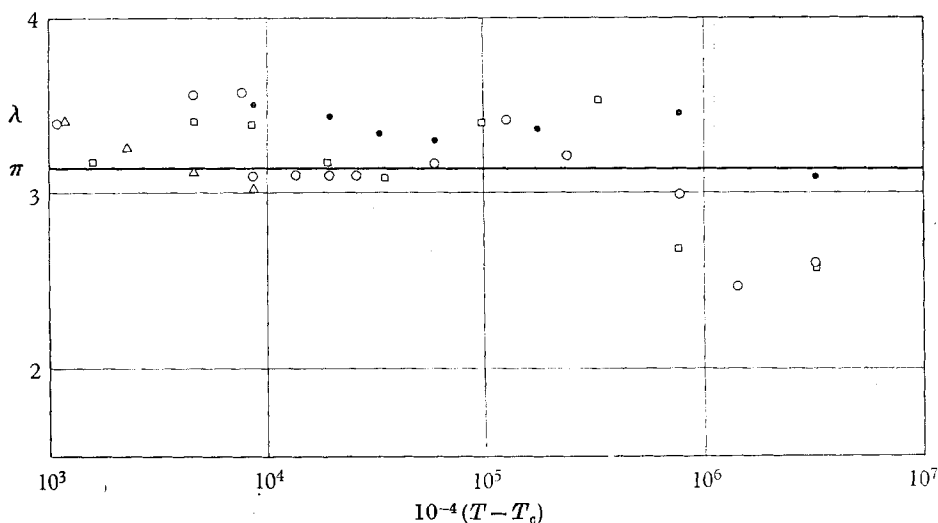


FIGURE 2. The dimensionless wave-number of the disturbance as a function of Taylor number. The various symbols denote the day on which the data was taken.

can be as large as 14%. But the Fourier analysis applied here reduces the statistical part of the error, and the averaging which results when a smooth line is drawn through the scattered points reduces the random error even more. Due to the large density of data points in figures 3-7 we believe that the statistical error in  $S$  has been reduced below 1%. Accordingly, we feel that the error in a line drawn through the data in figures 3-7 is not greater than 8%.

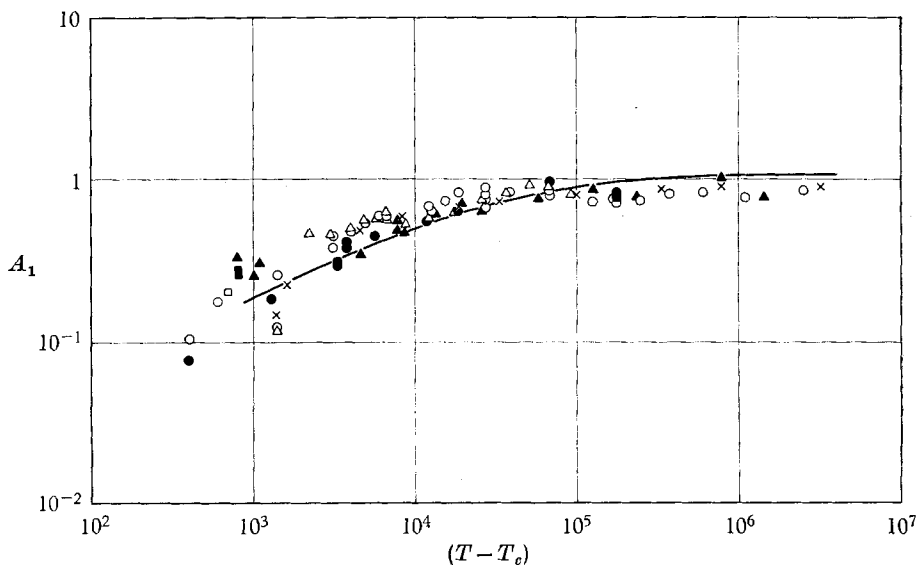


FIGURE 3. The amplitude of the fundamental in the Fourier analysis of the shear,  $A_1$  vs Taylor number. A new symbol is used for each day's data. The solid line is computed from Davey's tables.

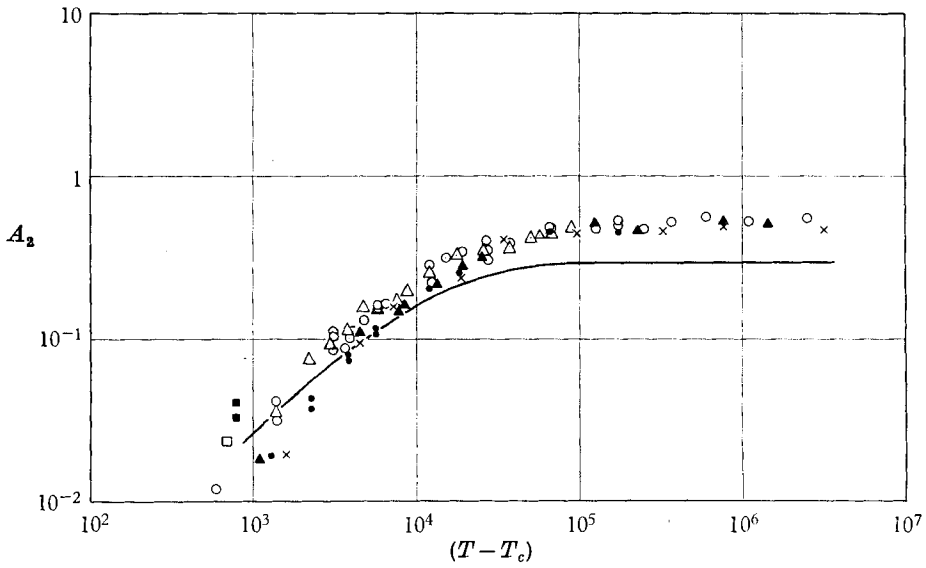


FIGURE 4. The amplitude of the first harmonic in the Fourier analysis of the shear  $A_2$  vs Taylor number. Different symbols refer to data taken on different days. The solid line is computed from Davey's tables.

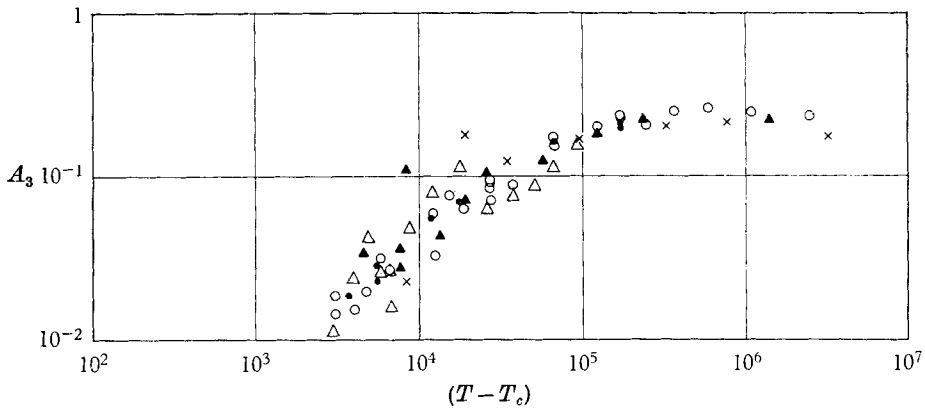


FIGURE 5. The amplitude of the second harmonic in the Fourier analysis of the shear  $A_3$  vs Taylor number. The symbol identifies the day the data was taken.

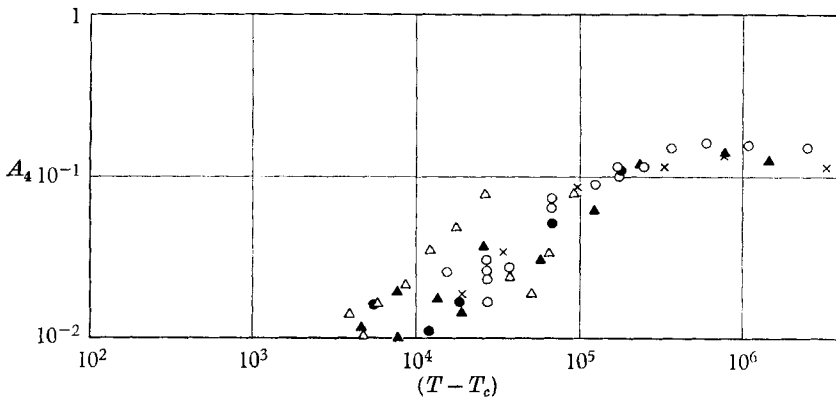


FIGURE 6. The amplitude of the third harmonic in the Fourier analysis of the shear  $A_4$  vs Taylor number. Again the symbol identifies the date of data taking.

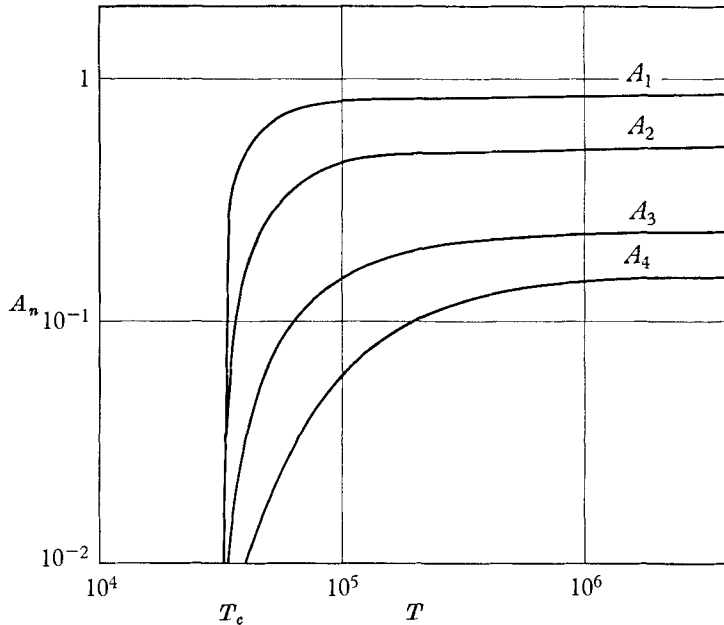


FIGURE 7. A comparison of the four Fourier components of the shear  $A_1$  through  $A_4$  at various Taylor numbers. The curves are smoothed forms of the experimental data on figures 3 through 6.

One out of the three thermistors has been used in taking almost all the data relating to amplitude. However, several runs have been made with the two other thermistors to show that the results are not dependent on the thermistor used. Considering the large systematic error that may occur in  $S$  it is encouraging that all of the resulting points fall within the scatter shown of figures 3–6. We wish to emphasize that there are no adjustable parameters in Davey's theory or in our own data.

Another result of the Fourier analysis is that up to  $100T_c$  none of the out-of-phase components of the harmonics ever become larger than the noise level as measured by the odd components. This means that simple Taylor cells are found over a very large range of Taylor numbers. Above  $100T_c$  an azimuthal dependence is added to the velocity field of the Taylor cell.\* The amplitude of the azimuthal part is small (of the order of 5% of the total amplitude), however, up to  $500T_c$ . We have not observed transition to turbulence up to  $500T_c$  in this apparatus.

## 6. Discussion

Two arguments against the validity of the experimental data are rather obvious. The first is that it is not evident *a priori* that the axial flow which is used to sweep the cells past the detector will not change these results. In answer we may state that experiments with various values of  $R_x$  have shown that any effect on  $\lambda$  and the  $A_n$ 's is nearly independent of  $R_x$  until  $R_x$  becomes about four times as large as the value used here. A detailed account of the Taylor problem with axial flow will be given at a later date.

\* Note added in proof: This has recently been shown to be caused by end effects.

A second criticism is that in measuring non-linear harmonic generation it is essential to insure that none of the harmonic content is due to the measuring instrument. The electronics, the thermistor characteristic, and the relation between shear and excess temperature are all non-linear. We have investigated the magnitude of harmonic generation in the electronics and the thermistor and find it to be negligible compared with hydrodynamic generation. Recall that both response curves are linear to 1% in the operating range. The non-linearity shown by equation (3.1) is compensated for by using (3.1) in the computation.

Davey (1962) made several assumptions in developing his theory. He treated  $\lambda$  as a constant and neglected all out-of-phase components of the harmonics. Both assumptions have been proved correct by the present research. We have seen that  $\lambda$  is constant up to about  $10T_c$  within the statistical scatter of the observations. At  $100T_c$  the value of  $\lambda$  differs from the value at critical  $\lambda_c$  by only 10%. Moreover, the averaged value of  $\lambda$  below  $10T_c$  corresponds to that used by Davey (1962). Also, the out-of-phase components of the harmonics are not larger than the noise level up to  $100T_c$ .

To compare the wave-function used by Davey (equation 2.2) with experiment it is necessary to measure all components of the Fourier series. The torque data indicates that the component  $A_0$  is predicted correctly. Our data extends the agreement to  $A_1$  and  $A_2$ . Experimental observations are on hand in figures 5 and 6 to compare  $A_3$  and  $A_4$  with theory. It would be desirable to extend Davey's computations to order  $A_e^4$  so that  $A_3$  and  $A_4$  may be compared. Each time the theoretical value of a Fourier component is found to agree with reality the degree of freedom of the unknown wave-form is reduced. It is difficult already with the first three components in agreement to construct a wave-function which is smooth and yet differs significantly from the wave-form of equation (2.2). It is evident from the agreement of  $A_0$ ,  $A_1$  and  $A_2$  to large values of  $T$  that higher-order terms such as  $a_2 u_{11}$ , etc., must be very small.

It is interesting to inquire how far up in Taylor number Davey's theory (1962) might be expected to apply. It certainly cannot be good above  $100T_c$  since Davey (1962) assumed that the wave-form has no  $\theta$ -dependence. The expansion method used by Davey does not contain a means of deciding what  $m\sigma$  should be compared with in determining whether it is large or small. Also, it is not clear theoretically if an expansion of  $\sigma$  in terms of  $(T - T_c)/T_c$  or  $(T - T_c)/T$  converges more rapidly at large  $T$ . Davey started with the former expression, which seems more natural, and derived a relation for  $\gamma$  and  $A_e$  in terms of  $T$  and  $T_c$  similar to equations (2.3) and (2.4). Later he replaced the former by the latter arguing that both are equivalent at small values of  $(T - T_c)$  where the theory is expected to hold. If  $A_e$  is calculated for large values of  $A_e$  using Davey's original expression, the agreement with theory holds only near  $T_c$ ; but using equations (2.3) and (2.4) we have fair agreement even to  $100T_c$ . It would be desirable to reformulate the theory so that  $(1 - T_c/T)$  is used in all expansions.

Within our limit of error, Davey's calculations agree with the experimental data up to about  $4T_c$ . This is probably as far as the theory may be expected to be strictly valid. Note that at  $4T_c$   $\lambda^2 \approx \sigma$ . For large values of  $T$  where the theory is

not expected to apply the discrepancy between theory and experiment is never greater than 40 %.

The truth of Davey's assumption that all harmonics of the axial periodicity add in phase plays an important role in the physical interpretation of the flow field. Davey's expansion for the velocity components  $u$  and  $v$  are of the form  $\Sigma_n B_n \cos n\lambda z$  and for the  $w$ -component  $\Sigma_n C_n \sin n\lambda z$ . The expansion for an idealized jet in the  $r$  or  $\theta$  directions centred at  $z = 0$  has the form of a delta function  $\Sigma_n \cos n\lambda z = \delta(\lambda z)$ ; the accompanying shock-like structure demanded by

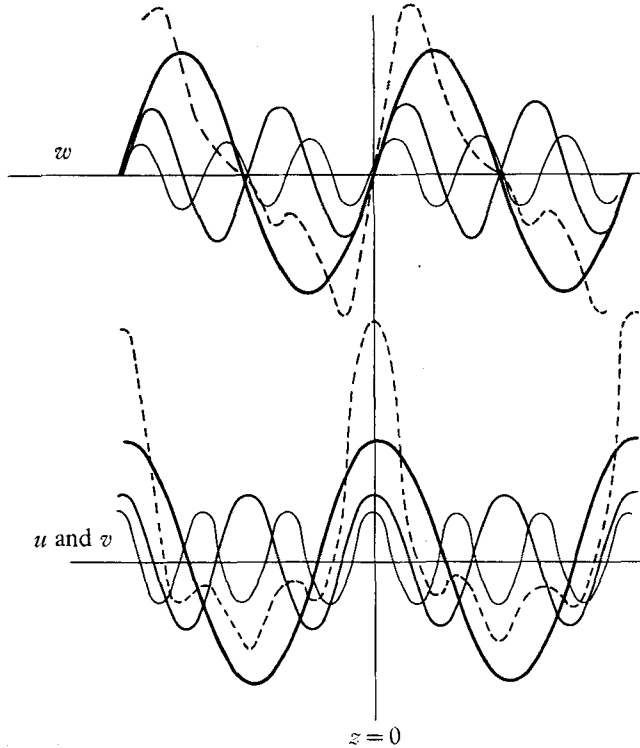


FIGURE 8. Summation of the harmonics to form jets in the  $u$  and  $v$  components and shock structure in the  $w$  component. The amplitudes have been estimated from the experimental data and are approximate.

continuity has the form  $\Sigma_n n^{-1} \sin n\lambda z$ . Visual observations suggest that as  $T \rightarrow \infty$  it is possible that both  $u$  and  $v$  are approaching ideal jets and that  $w$  is a sawtooth wave as a function of  $z$ . This would require in Davey's expansion that  $B_n \rightarrow 1$  and  $C_n \rightarrow 1/n$  as  $T \rightarrow \infty$ . Our data shown in figure 7 indicates that the  $A_n$ 's approach constant values asymptotically as  $T \rightarrow \infty$ . If we assume that for  $T \gg T_c$ ,  $B_n = 1$  and  $C_n = 1/n$ , then the  $A_n$ 's calculated from equation (2.8) and (2.9) are in agreement with the four measured values of  $A_n$  at large  $T$ . It does not appear that it has been fully appreciated that Davey's wave-function allows jets and shock-like structure. In figure 8 the approximate experimental values of the first three harmonics are added together for  $T \approx 8T_c$  to show the build up of jets and shocks. (The values of figure 8 are estimated since it is very difficult to get the harmonics from the  $A_n$ 's.)

The schematic diagram figure 9 shows how a pair of Taylor cells which are symmetrical at transition are distorted by finite-amplitude effects. The centres of circulation in the axial plane of each of the two cells making up a pair move closer together as  $T$  is increased. The back flow becomes slow and occupies most of the cell. The jet is formed at the cell boundary and is always outward from the inner cylinder—this is in agreement with Davey's theory. Note that there is also a jet in the  $v$  direction. It is possible to observe the cells visually using ink as a tracer. The streamlines are similar to those shown in figure 9 and the jets are quite definite. Since the centrifugal force is the only unsymmetrical force in the axial plane, it is probably the cause of the jet.

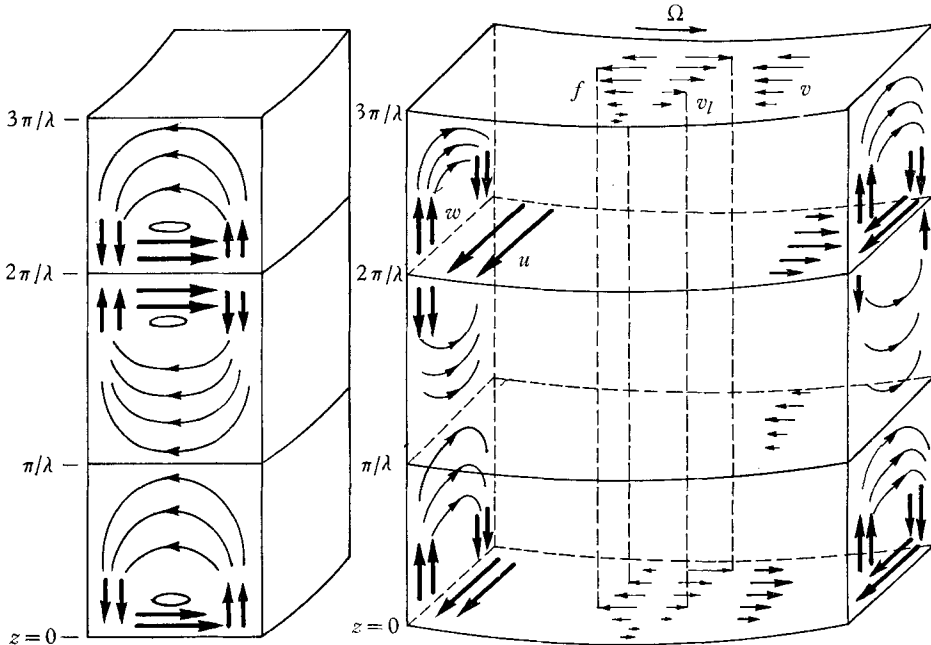


FIGURE 9. A schematic picture of the Taylor cells at about  $10T_c$ , showing the distortion of the cell due to finite-amplitude effects.

It would be interesting to carry out an analysis of the limiting form of Taylor cells as  $T \rightarrow \infty$ . The boundary-layer approach proposed by Batchelor (1956) should apply. However, it is now obvious that the cells must be treated in pairs—not individually.

The jet might be expected to produce an excess pressure on the outer cylinder where it impinges: the velocity of the jet is of the order of 5 cm/sec (from figure 3 and actual values of  $R_1$  and  $\nu$ ) so that the Bernoulli pressure at stagnation should be about 0.1 mm of the liquid. An attempt to measure this pressure in another Taylor double-cylinder apparatus failed. A standpipe manometer was fitted to the outer cylinder of the apparatus. The height of the liquid level between the cylinders was adjusted so that the jet was either at the entrance to the standpipe or far from it. The differential pressure due to rotation was measured in each case, but the effect of rotation was negligible. The noise level was about 0.1 mm so that it is not surprising that the result was negative.



A few traces of the wave-form such as figure 1 were made with the anemometer mounted on the inside of the outer cylinder. The jets were less sharp for corresponding Taylor numbers than those of figure 1. This is in accordance with Davey's computations (1962). It appears that the jet does not exert an appreciable force on the outer cylinder at the point of impact.

In the course of the experiments reported in this paper and in other work with this apparatus evidence has frequently appeared which could be construed as indicating the existence of another type of instability near  $T_c$ . The critical Taylor number has been determined by plotting  $A_1^2$  vs  $T$  and also  $A_2$  vs  $T$  in the vicinity of  $T_c$ . For acceptable data both curves are straight lines and their intercepts with the  $T$  axis differ by less than 2%. Using this value for  $T_c$ , we always find a large scatter of points near  $T_c$  (up to 3% above) on an  $A_n$  vs  $(T - T_c)$  plot. The points which do not fall on a smooth curve are consistently high—the cells appear below critical or have an amplitude higher than expected. The same effect occurs in the data of Donnelly & Schwartz (1965) using the ion technique and also in the torque data of Donnelly (1958). We also observe that the wavelength of those cells, which appear prematurely, are always considerably larger than (up to two times) the observed value of  $\lambda$  extrapolated to  $T_c$  from above would imply.

## 7. Conclusion

These experiments show that the methods of treating finite-amplitude secondary flows proposed by Stuart (1958, 1960) and by Watson (1960) and applied to the Taylor problem by Davey (1962) yield accurate results. Our data, which may be in error by 8%, agrees with the calculations up to  $4T_c$ . Two results of this research are important in considerations of geophysical fluid dynamics. First, the data proves that secondary flows of simple wave-form can occur over very large ranges of Taylor number in rotating systems. Secondly, it is shown that the non-linearity of the equations of motion is a sufficient mechanism to produce jets in simple types of fluid flow.

We wish to acknowledge helpful discussions concerning this work with Dr J. T. Stuart, Dr R. C. Di Prima, and Dr L. A. Segel. The apparatus for these experiments was constructed as a joint venture with Dr S. K. F. Karlsson. The research reported in this paper was sponsored in part by The Air Force Cambridge Research Laboratories, Office of Aerospace Research, under contract no. AF19(628)-4783 and in part by The National Science Foundation under grant GK 168.

## REFERENCES

- BATCHELOR, G. K. 1956 *J. Fluid Mech.* **1**, 177.  
 CHANDRASEKHAR, S. 1961 *Hydrodynamic and Hydromagnetic Stability*. Oxford: Clarendon Press.  
 COLES, D. 1965 *J. Fluid Mech.* **21**, 385.  
 DAVEY, A. 1962 *J. Fluid Mech.* **14**, 336.  
 DI PRIMA, R. C. 1963 *J. Appl. Mech.* **30**, 486.  
 DONNELLY, R. J. 1958 *Proc. Roy. Soc. A*, **246**, 312.

- DONNELLY, R. J. & SCHWARTZ, K. W. 1965 *Proc. Roy. Soc. A*, **283**, 531.
- DONNELLY, R. J. & SIMON, N. J. 1960 *J. Fluid Mech.* **7**, 401.
- KARLSSON, S. K. F. & SNYDER, H. A. 1965 *Ann. Phys. N.Y.* **31**, 314.
- LAMBERT, R. B., SNYDER, H. A. & KARLSSON, S. K. F. 1964 *Phys. Letters*, **9**, 229.
- LAMBERT, R. B., SNYDER, H. A. & KARLSSON, S. K. F. 1965 *Rev. Scient. Instrum.* **36**, 924.
- NILNER, P. P. 1965 *Rev. Scient. Instrum.* **36**, 921.
- SNYDER, H. A. 1962 *Proc. Roy. Soc. A*, **152**, 198.
- SNYDER, H. A. & KARLSSON, S. K. F. 1964 *Physics. Fluids* **7**, 1696.
- SNYDER, H. A. & KARLSSON, S. K. F. 1965 *Ann. Phys. N.Y.* **31**, 292.
- STUART, J. T. 1958 *J. Fluid Mech.* **4**, 1.
- STUART, J. T. 1960 *J. Fluid Mech.* **9**, 353.
- TAYLOR, G. I. 1923 *Phil. Trans. A*, **223**, 289.
- TAYLOR, G. I. 1936 *Proc. Roy. Soc. A*, **157**, 546.
- WATSON, J. 1960 *J. Fluid Mech.* **9**, 371.
- WENDT, F. 1933 *Ingen-Arch.* **4**, 577.